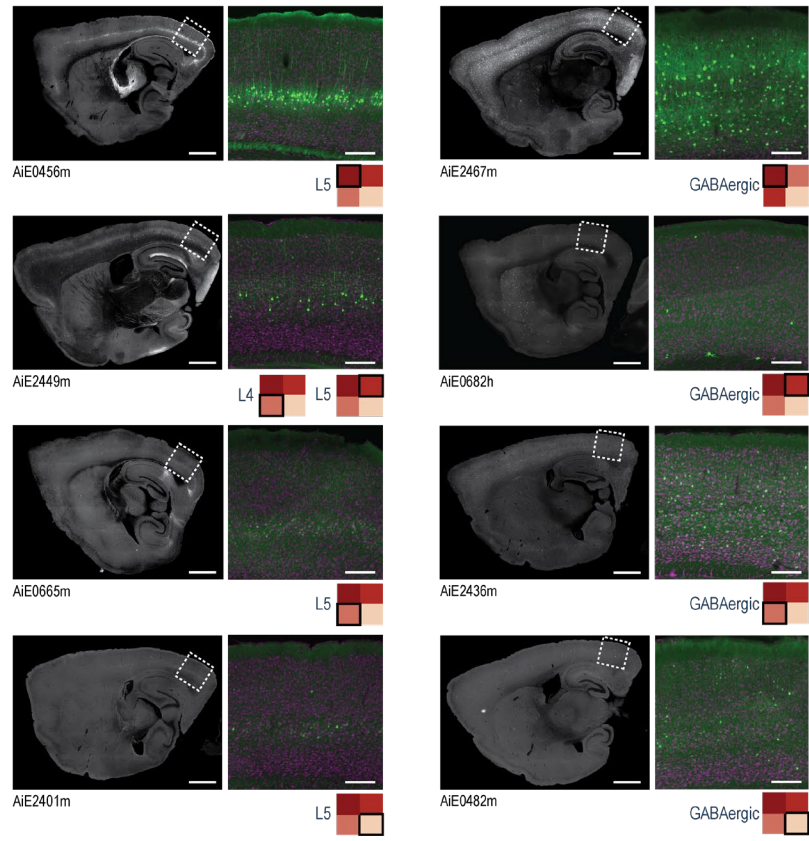


Figure S1: Analysis of sequence alignment across species. A. Histograms showing the proportion of mouse (grey) and human (blue) sequences, according to their length along with a histogram showing the length distribution of the liftover sequences (full green). Bin size = 50 bp. **B.** Histogram of the sequence homology, calculated as the total number of identical base pairs (liftover length x percent identity) of the total length of the original enhancer sequence. Bin size = 2%. **C-E.** Correlation analysis between the conservation of accessibility and the percent identity between the overlapping sequence only (C), overlap length (D) and the sequence homology relative to the length of the original sequence (E). Linear fit lines are shown in red, and the Pearson's coefficient with its p-value are shown at the bottom right corner of each plot.

A



B

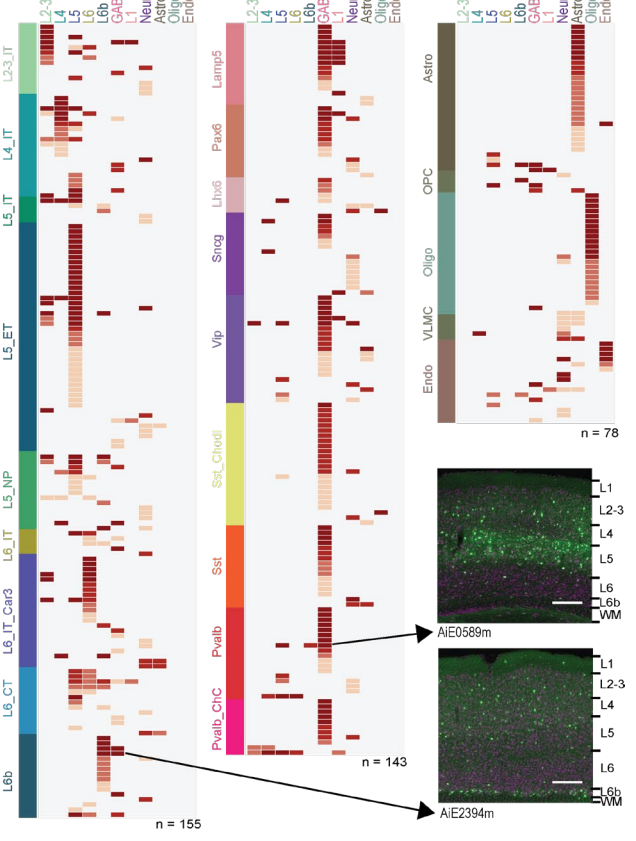


Figure S2: Enhancer scoring based on epifluorescence image sets. A. Representative sagittal images from eight experiments with focus on two cell categories: L5 (left column) or GABAergic (right). Scoring according to the scheme in Figure 3B is shown below each set of images. **B.** A heat map of all enhancers evaluated, which produced any labeling in the neocortex, arranged according to the cell population where their accessibility was highest, showing the identity of the labeled cell population and the labeling quality, according to the scheme in Figure 3B. The number of individual experiments in each category is shown below each plot (total n = 376). For images, scale bars for full section and expanded views are 1.0 and 0.2 mm, respectively.

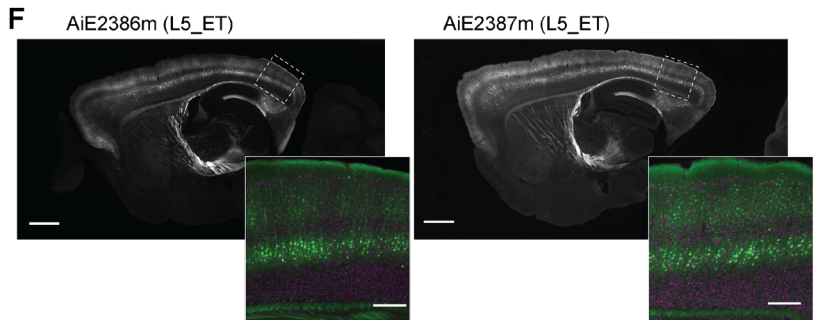
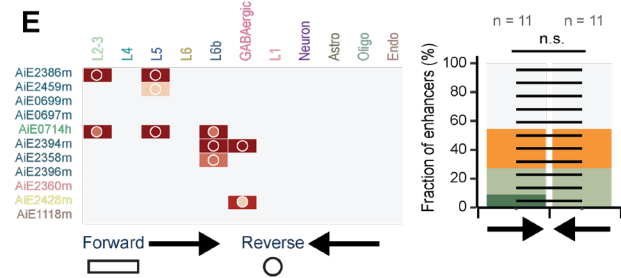
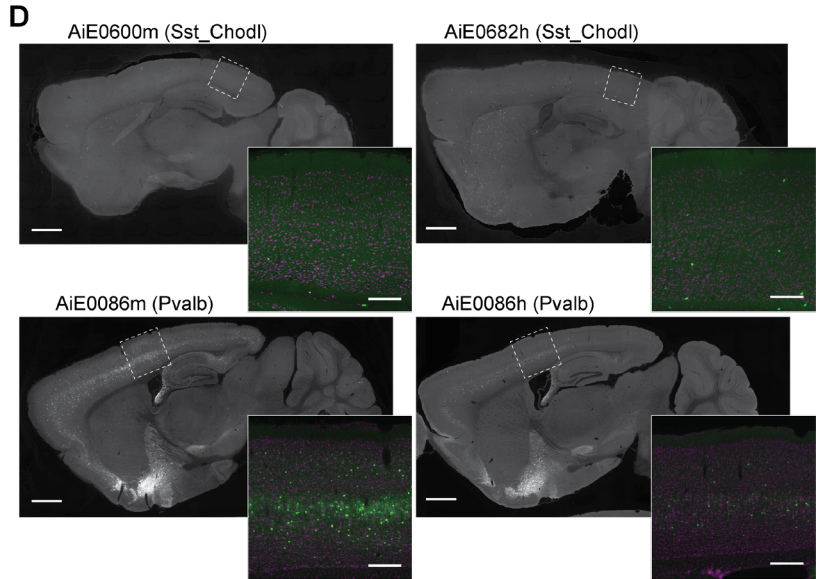
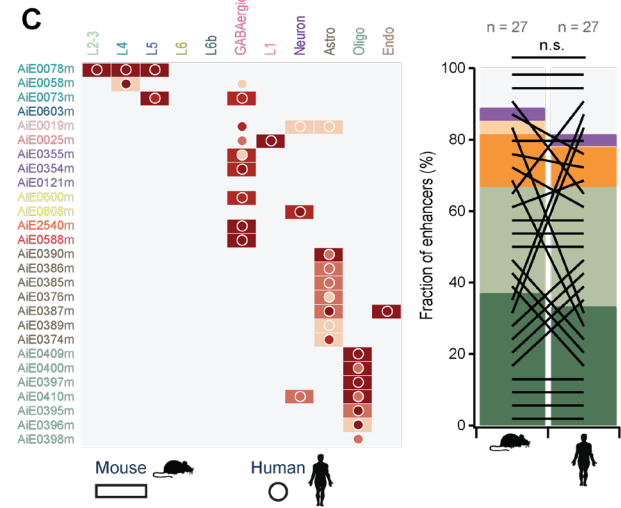
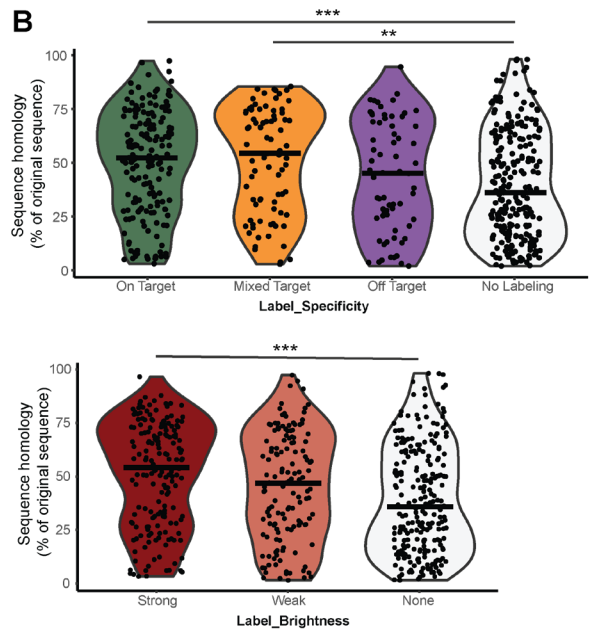
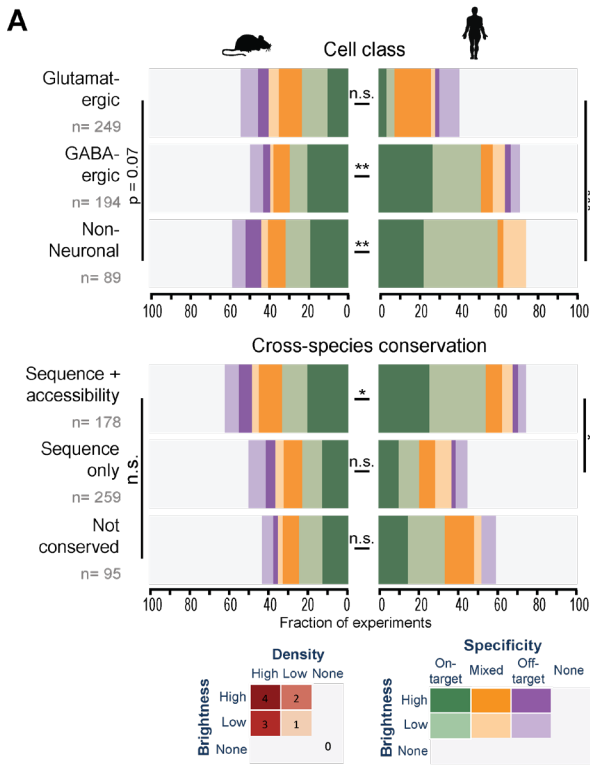


Figure S3: Effects of cross-species conservation and sequence orientation on enhancer performance.

A. Summary plot of enhancer scoring data according to their genome of origin (top) and cross-species conservation of sequence and accessibility (bottom). **B.** Violin plots showing the degree of mouse-human sequence homology according to the different specificity (top) and brightness (bottom) categories. P-values were calculated with one-way ANOVA, followed by a pairwise post-hoc analysis (Tukey) corrected for multiple comparisons (Bonferroni). Significance levels are the same as in (A). **C.** Summary plot of the scoring data for mouse (rectangles) alongside its human (circles) orthologous sequence (Left) and a summary plot of the scoring data according to the brightness and specificity, with black lines connecting each pair (Right). **D.** Representative epifluorescence images of sagittal sections, showing labeling pattern for two individual mouse enhancers (left) and their human orthologs (right). **E.** Summary plot of the scoring data for complementary oriented sequences (left) and a summary plot of the scoring data according to the brightness and specificity, with black lines connecting each pair (right). **F.** Representative epifluorescence images of sagittal sections, showing identical labeling pattern for a complementary pair. P-values were calculated using a chi-squared test. P-values < 0.05, < 0.01 and < 0.001 are denoted by *, **, ***, respectively, n.s. = not significant. Scale bars for full section and higher-magnification view = 1.0 and 0.2 mm, respectively.

Figure S4: Distribution of specificity and brightness across enhancer AAVs. **A.** Representative plots of the FACS gating strategy for selective collection of cells labeled by the Lamp5 enhancer AiE2103m: Forward (FSC-A) and side scatter (SSC-A) were used to select objects matching size and granularity of cortical cells (left) and this fraction was further separated according to signal detected in the DAPI and FITC channels (right), in order to avoid collection of DAPI+ cells, whose membrane is likely compromised. Dashed boxes indicate the gates applied for sample collection. **B.** Box plots showing the distribution of enhancer maximum specificity in each of the cortical clusters. **C.** A cumulative distribution plot showing the fraction of enhancers as a function of their specificity, estimated by the maximal fraction of labeled cells. **D.** A cumulative distribution plot showing the fraction of enhancers as a function of their brightness, relative to hSyn1. **E.** A cumulative distribution plot showing the fraction of enhancers as a function of correlation coefficient, between the distribution of labeled cells and distribution of chromatin accessibility, across the cortical subclasses. **F.** Cross-correlation plot showing correlation values (white-green scale, bottom left corner) and their respective p-values (blue-orange scale, top right corner). Dashed lines in plots (A-C) show the median and top 10th percentile of enhancers. P-values in (D) were corrected for multiple comparisons.

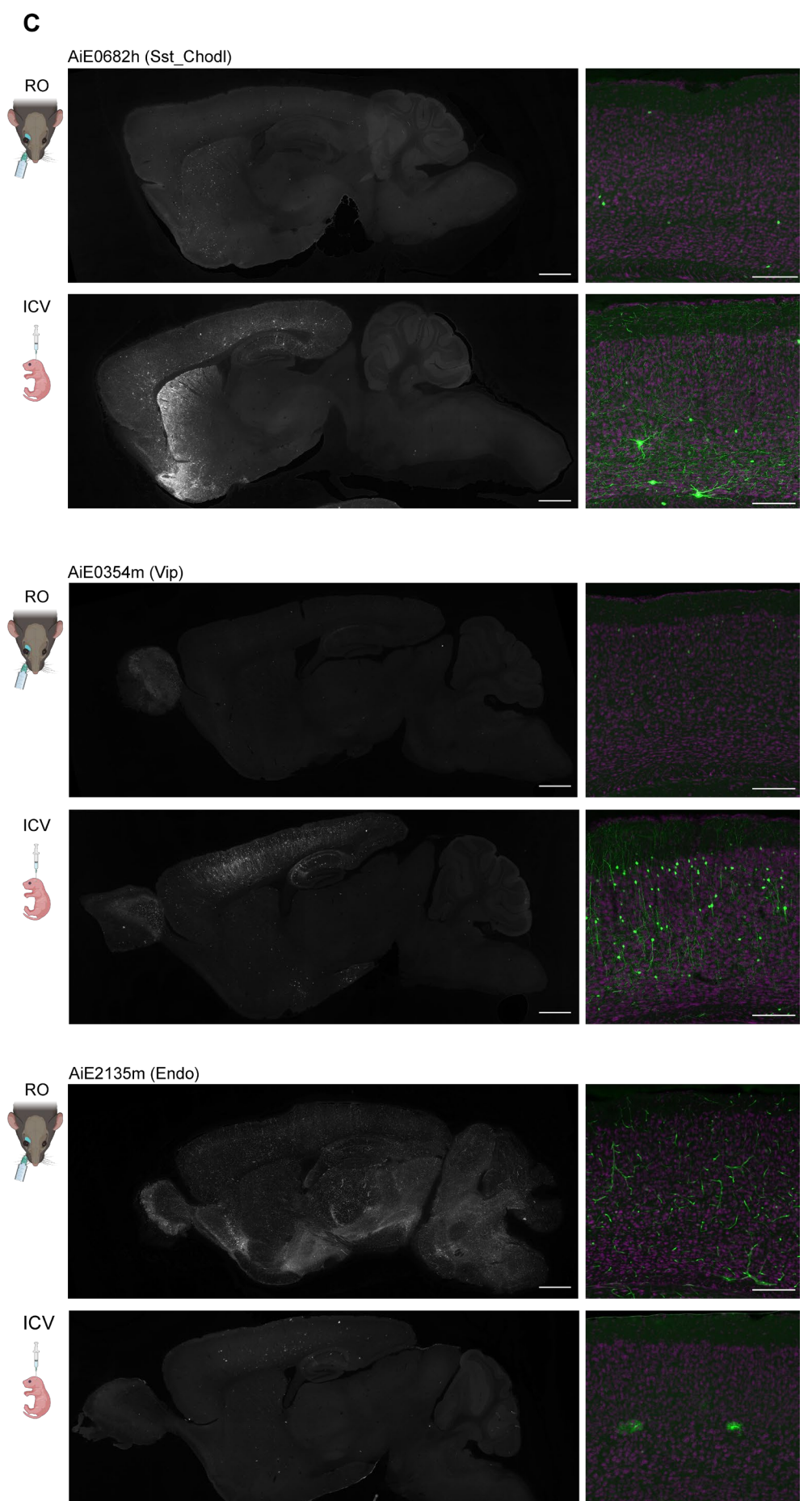
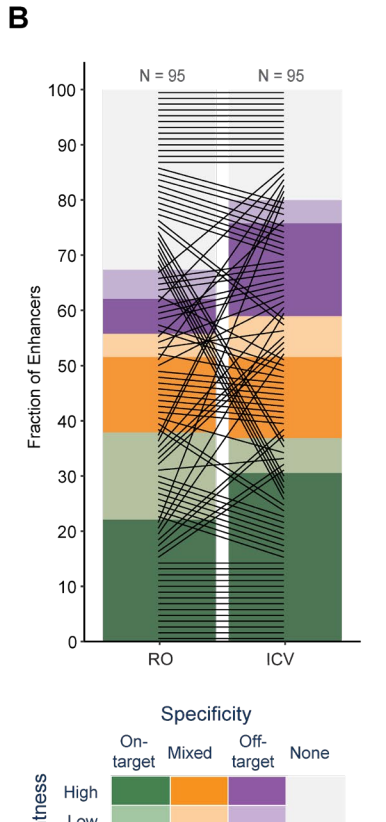
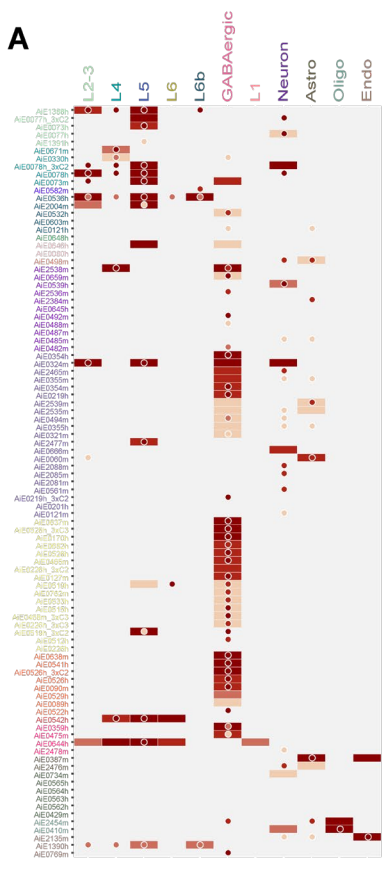


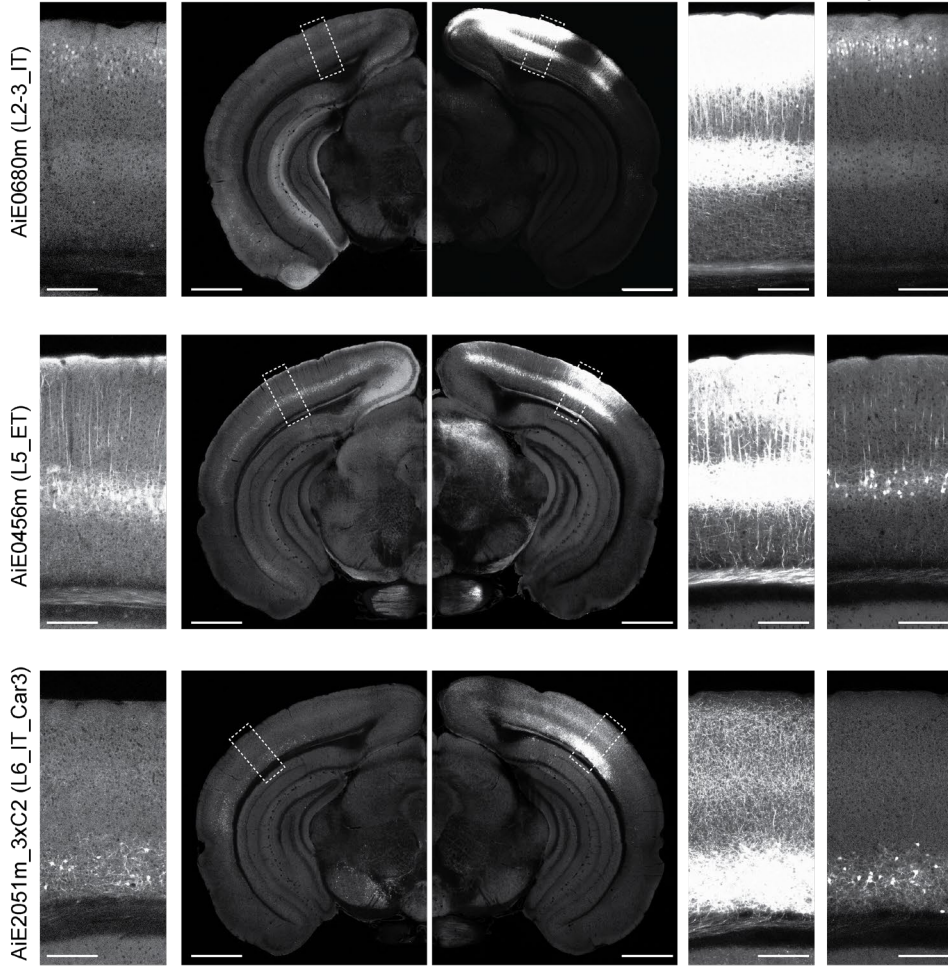
Figure S5: Comparison RO and ICV viral delivery routes by image scoring data. **A.** Heatmap of scoring data for the same vectors, delivered RO (rectangles) or ICV (circles). **B.** Summary plot of the scoring data according to the brightness and specificity, with black lines connecting each pair. **C.** Representative epifluorescence images of sagittal sections of three individual enhancers, comparing labeling pattern when the virus was delivered via the RO (top) or ICV (bottom) route. An expanded view of the visual cortex is displayed to the right of the full-sized image. Scale bars for full section and expanded view = 1.0 and 0.2 mm, respectively.

A

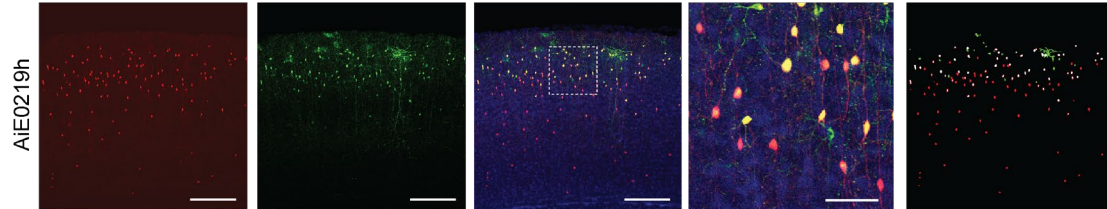
Retro-orbital
(5×10^{11} gc in 90 μ l PBS)

Stereotaxic
(1.5×10^9 gc in 0.3 μ l PBS)

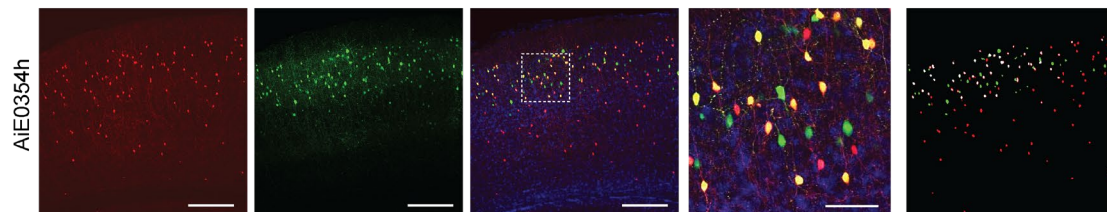
Brightness adjusted

**B**

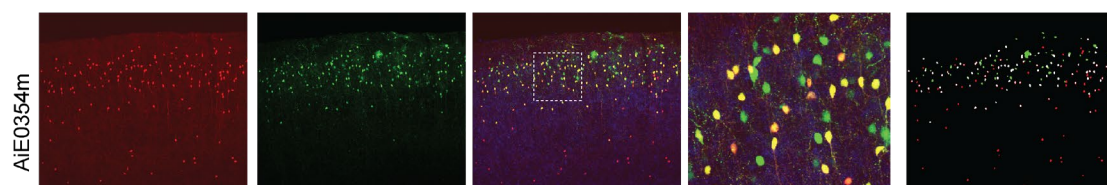
Vip-IRES-cre;Ai14 SYFP2 Merge Mask



Completeness: 50%
Specificity: 78%
Specificity (SSv4): 84%



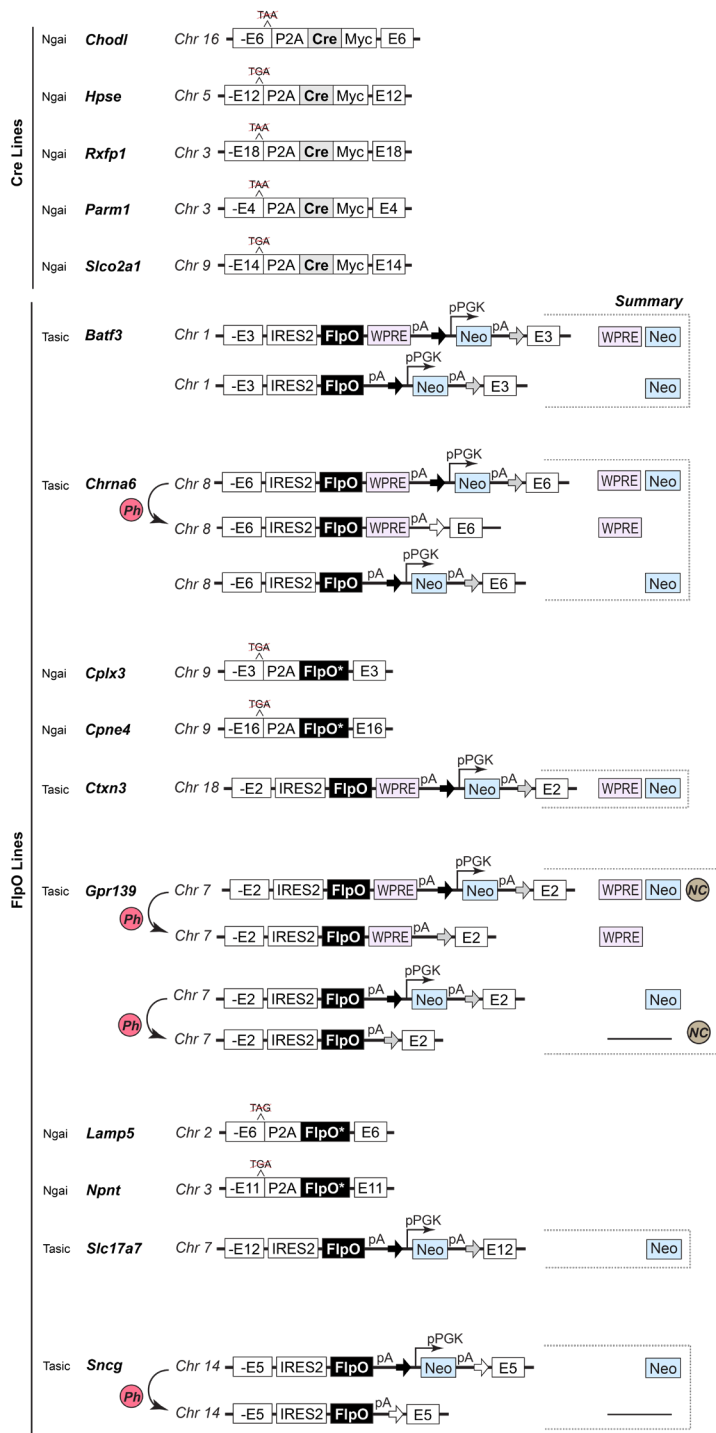
Completeness: 47%
Specificity: 56%
Specificity (SSv4): 82%



Completeness: 65%
Specificity: 69%
Specificity (SSv4): 77%

Figure S6: Stereotaxic delivery of enhancer AAVs. A. Stereotaxic delivery into VISp of three enhancers AAVs targeting different subclasses of glutamatergic neurons, resulted in strong, layer restricted SYFP2 expression. Scale bars for full section and expanded view = 1.0 and 0.2 mm, respectively. **B.** Stereotaxic delivery of three enhancers targeting Vip interneurons (green), delivered to the VISp of *Vip-IRES-Cre;Ai14* double transgenic line (red). For each injection, completeness was calculated as the fraction of SYFP2⁺/tdTomato⁺ cells, of all tdTomato⁺ cells at the injection site, and specificity was calculated as the fraction of SYFP2⁺/tdTomato⁺ cells, of all SYFP2⁺ cells. Specificity results were compared with SSv4 measurements for each vector, following RO delivery of 5x10¹¹ genome copies (gc). n = 1 experimental animal for all experiments shown in this figure. Scale bars for full VISp view and expanded view = 0.2 and 0.05 mm, respectively.

A Driver lines; alleles made by knock-in



B Reporter lines; Chr. 9, TIGRE locus; made by Bxb1 integrase-mediated cassette exchange into a landing-pad ES cell line

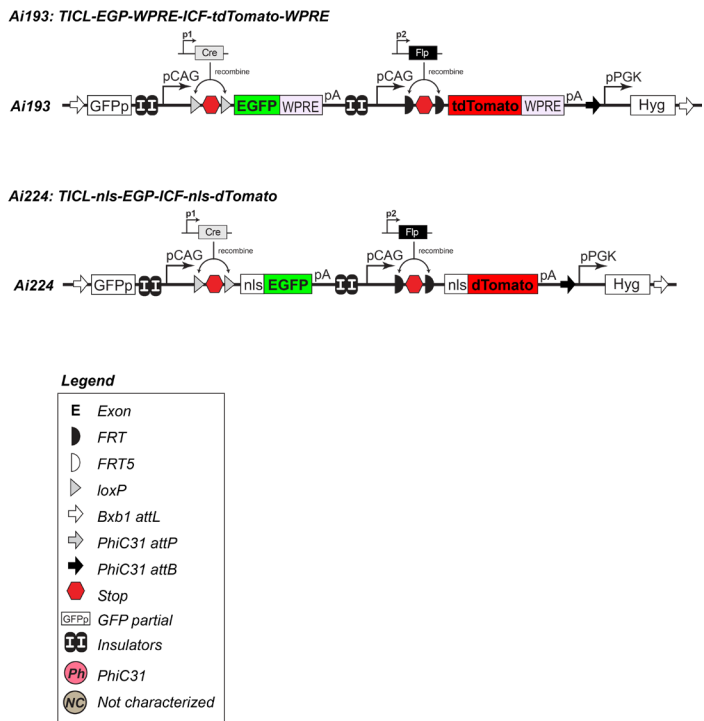


Figure S7: Transgenic line designs. A. Schematics depicting design of the 15 driver lines. Of these, five express Cre recombinase whereas 10 express FlpO. For some lines, such as *Chrna6-IRES2-FlpO*, we have versions with WPRE, with Neo present as well as with Neo removed allowing us to compare expression patterns in all three. In some instances, the driver lines were used as is and in others, they were crossed with *Rosa26-PhiC31* mice to delete the pPGK-neo selection cassette. **B.** Schematic depicting the design of the two new reporter mice *Ai193* and *Ai224*.

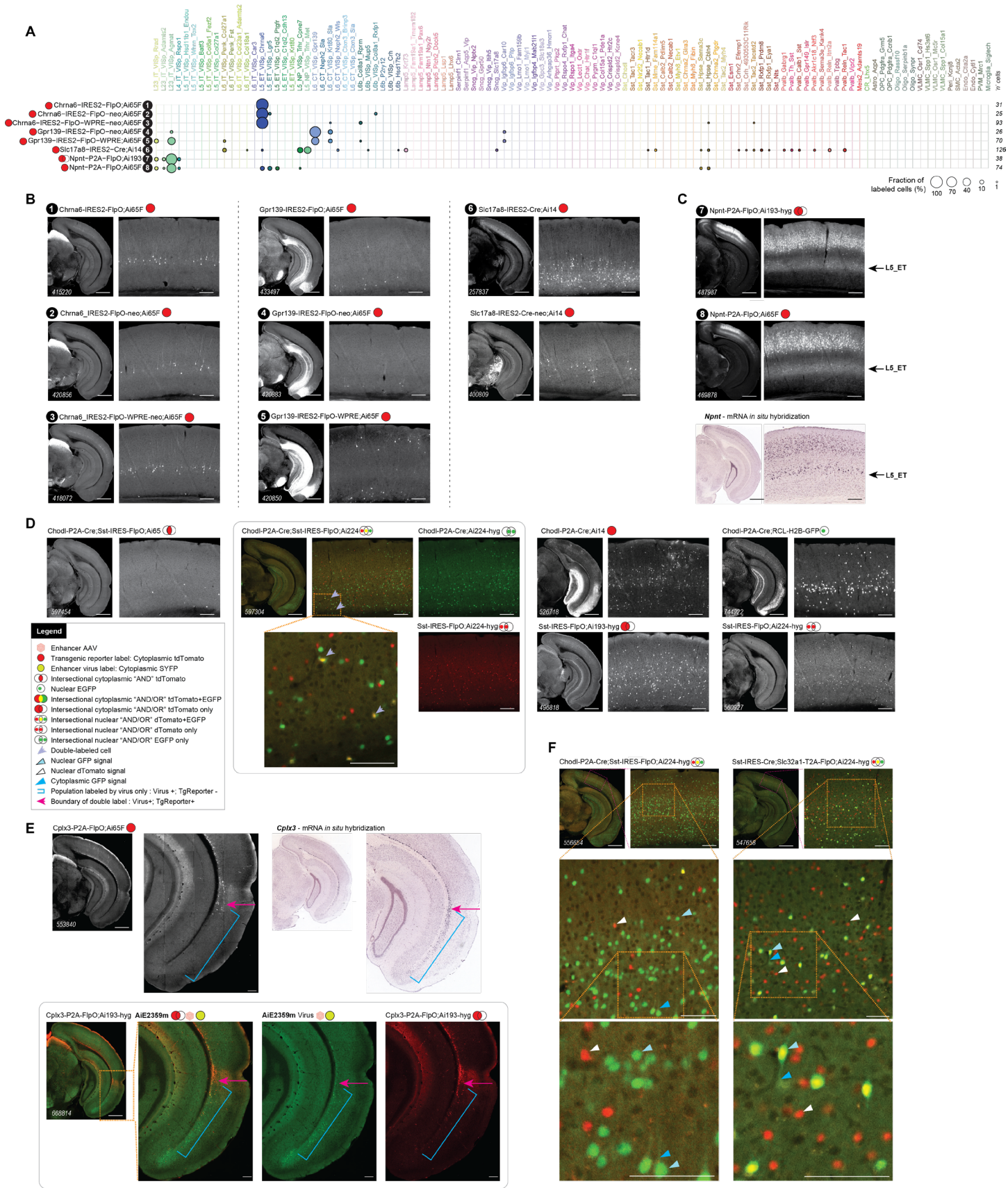


Figure S8. Factors influencing tool expression and evaluation. **A.** scRNA-seq (SSv4) data showing distribution of labeled cells from tools **1-8** mapped to mouse VISp taxonomy and displayed at the cluster level. **B.** Select STPT images for tools **1-6**, and additional related tools. **C.** Representative *Npnt* mRNA *in situ* hybridization and STPT images of *Npnt-P2A-FlpO* with two different reporters showing labeling of cells in L5, whereas the SSv4 data for the cross to *Ai193* (tool **7** in A) do not show L5 cells. This could be due to L5_PT cells not surviving FACS for this experiment. **D.** Representative STPT data for *Chodl-P2A-Cre; Sst-IRES-FlpO* crossed with previously characterized reporters (*Ai14* and *Ai65F*) and the new AND/OR reporters (*Ai193* and *Ai224*) both independently and as a triple transgenic. **E.** Representative STPT images showing *Cplx3-P2A-FlpO* with different reporters and *Cplx3* mRNA expression (blue brackets) by RNA *in situ* hybridization (<https://mouse.brain-map.org/experiment/show/70928340>). The expression pattern for the enhancer AAV, AiE2359m, mirrors *Cplx3* expression (blue brackets) by RNA *in situ* hybridization, whereas the expression of the transgenic line, *Cplx3-P2A-FlpO;Ai193* does not include *Cplx3*⁺ cells in the entorhinal area. **F.** Expression of nls-EGFP (Cre-dependent) and nls-dTomato (Flp-dependent) is faithful in the *Ai224* reporter line; however, nuclear localization is imperfect. The GFP appears mostly nuclear, but weak signal can be observed in the cytoplasm (light blue arrow) and processes (blue arrow). In comparison, nls-dTomato appears nuclear (white arrow). Scale bars: 1.0 and 0.2 mm for full section and expanded view; 0.1 mm for further expanded view in (C).